



Radiative model for the microquasar SS433: Non-thermal emission from the eastern jet

P. Sotomayor Checa^{1,2} & G.E. Romero^{1,2}

¹ *Instituto Argentino de Radioastronomía, CONICET-CICPBA-UNLP, Argentina*

² *Facultad de Ciencias Astronómicas y Geofísicas, UNLP, Argentina*

Contact / psotomayor@iar.unlp.edu.ar

Resumen / En este trabajo proponemos un modelo leptó-hadrónico para la emisión no térmica del jet oriental del microcuásar galáctico SS433. Obtenemos que el flujo en TeV reportado por la Colaboración HAWK puede explicarse por el decaimiento de piones neutros producidos en colisiones inelásticas protón-protón. La emisión en radio y rayos X es correctamente modelada por radiación sincrotrón de electrones relativistas primarios.

Abstract / In this work we propose a lepto-hadronic model for the non-thermal emission of the eastern jet of the galactic microquasar SS433. We obtain that the flux in TeV reported by the HAWK Collaboration can be explained by the decay of neutral pions produced in inelastic collisions proton-proton. Radio and X-ray emission is correctly fitted by synchrotron radiation of relativistic primary electrons.

Keywords / radiation mechanisms: non-thermal — stars: individual (SS433) — X-rays: binaries

1. Introduction

Microquasars are binary systems composed of a normal star and a compact object (a neutron star or a black hole), linked gravitationally (Mirabel & Rodríguez, 1994). In these sources, material from the star is accreted by the compact object, and an accretion disk is formed that radiates a fraction of the gravitational energy of the captured matter. Close to the accreting object, powerful relativistic jets of matter and radiation are launched, perpendicular to the orbital plane.

The binary SS433 is a well-known microquasar for its precessing, mildly relativistic, highly-collimated, and baryon-loaded jets (Abell & Margon, 1979; Margon, 1984; Eikenberry et al., 2001; Marshall et al., 2002; Fabrika et al., 2007). This source is the only super-accreting object known in the Galaxy (Shkrovskii, 1981). The donor star and the compact object are surrounded by a precessing accretion disk. The material in this envelope comes from the wind from the accretion disk (Fabrika, 1993). The existence of an equatorial wind in SS433 has been revealed by high-resolution radio interferometric observations (see e.g. Blundell et al., 2001; Paragi et al., 2002).

The non-thermal Galactic radio nebula W50 surrounds the central source of SS433 (Geldzahler et al., 1980; Downes et al., 1981; Elston & Baum, 1987). In the region of interaction between W50 and the jets of SS433, acceleration of relativistic particles is expected, probably by a first-order Fermi mechanism (Dubner et al., 1998). The radio emission regions are spatially coincident with lobes observed in X-rays (Safi-Harb & Ögelman, 1997).

Recently, the HAWK Collaboration has reported a gamma-ray flux with energies of at least 25 TeV from

the SS433/W50 system spatially resolved in the lobes. This emission has been explained as inverse Compton scattering of relativistic electrons that also produce radio and X-ray emission (Abeysekara et al., 2018).

In this work we show that the emission reported by the HAWK Collaboration can also be explained by the decay of neutral pions produced in inelastic collisions pp , in agreement with the data observed at other wavelengths.

2. Model

We adopt a lepto-hadronic model for the emission from the brightest X-ray knot, indicated as “e2” in Figure 1 of Abeysekara et al. (2018), which shows a gamma-ray image of the SS433/W50 region.

We consider that a population of electrons and protons are injected following a power-law type function in the energy $Q_{e,p}(E) = K_{e,p}E^{-p_{inj}}$, where $K_{e,p}$ is the normalization constant. The radiative processes by which electrons are cooled are: synchrotron radiation, inverse Compton scattering, and relativistic bremsstrahlung radiation. In the case of protons, the radiative losses are because of synchrotron radiation, inelastic collisions pp , and photo-hadronic interactions. The target photon field for both electron and proton interactions is the cosmic microwave background (CMB). We also consider adiabatic losses produced by the expansion of the cooling region. Particle escape is introduced through Bohm diffusion, which constitutes a conservative hypothesis.

To test our model we proceed as explained below. We solve the transport equation for injected relativistic particles assuming a one-zone model. We thus obtain the distribution of relativistic particles in the emission

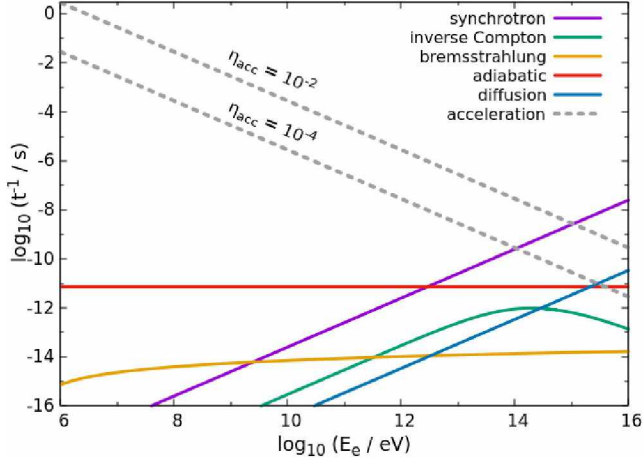


Figure 1: Timescales for relativistic electrons.

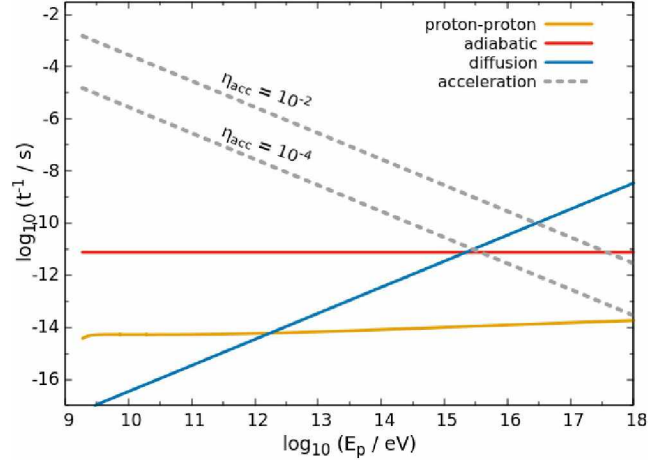


Figure 2: Timescales for relativistic protons.

region. We calculate the emissivities in the comoving frame, and applying the appropriate relativistic transformations we obtain the spectrum emitted in each radiative process in the frame of the observer. Finally, we plot the observational data and calibrate the free parameters of the model.

Detailed formulas for calculating the spectrum of photons emitted from the particle injection function can be found in Reynoso et al. (2008, 2011); Romero & Vila (2008); Romero et al. (2010); Sotomayor Checa & Romero (2019) and references therein. The parameters used in our model are listed in Table 1.

Table 1: Parameters of the model.

Parameter [Unit]	Value
L_{jet} : Jet kinetic power [erg s^{-1}]	2×10^{39}
L_p : Power in relativistic protons [erg s^{-1}]	2×10^{38}
L_e : Power in relativistic electrons [erg s^{-1}]	4×10^{35}
B : Magnetic field in the knot [R_\odot]	3×10^{-5}
n : Density in the optical filaments [cm^{-3}]	4
p_{inj} : Spectral index for the injection [R_\odot]	1.9
R_{knot} : Knot size [pc]	8
η_{acc} : Acceleration efficiency	10^{-2}

3. Results

We show the cooling and acceleration timescales for electrons and protons in Figures 1 and 2. For electrons, adiabatic and synchrotron cooling are the dominant loss processes. Equating the synchrotron cooling and acceleration rates $t_{\text{synchr},e}^{-1} = t_{\text{acc},e}^{-1}$, we obtain the maximum energy of the electrons $E_{\text{max},e} = 1.1 \times 10^{15}$ eV.

If the acceleration of protons is efficient, their maximum energy is limited by diffusive escape. If the acceleration is inefficient, their maximum energy is determined by adiabatic losses. In this work, efficient acceleration is assumed for both electrons and protons. Setting $t_{\text{diff}}^{-1} = t_{\text{acc}}^{-1}$, we then obtain $E_{\text{max},p} = 2.9 \times 10^{16}$ eV.

The spectrum of electrons and protons in the region of emission is shown in Figures 3 and 4. In both cases, a change in the slope of the distribution function is observed in the energy value corresponding to the change in the dominant cooling/escape process.

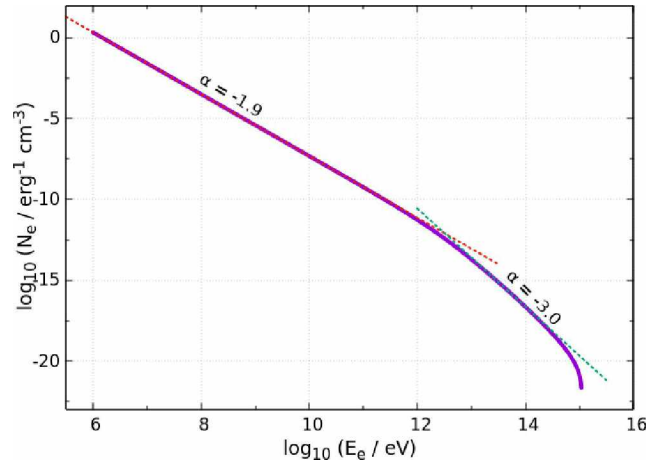


Figure 3: Distribution of relativistic electrons.

The broadband spectrum of non-thermal radiation is presented in Figure 5. Radiative processes that are not shown in the final spectrum do not contribute significantly to the flux observed at any wavelength. We find that our lepto-hadronic model can reproduce the observed data according to current observational constraints. We have considered the data provided in Geldzahler et al. (1980); Safi-Harb & Petre (1999); Brinkmann et al. (2007); MAGIC Collaboration et al. (2018) and Abeysekara et al. (2018).

4. Conclusions

In this work we propose a lepto-hadronic model for the eastern jet of SS433 in order to explain the observed

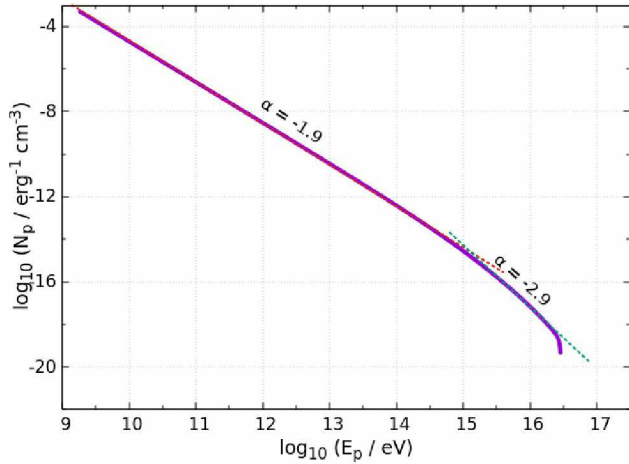


Figure 4: Distribution of relativistic protons.

data. We consider an injection of relativistic particles with an spectral index consistent with the prediction by the diffusive shock acceleration theory. An efficient acceleration mechanism is adopted and Bohm diffusion is the escape process assumed. We obtain that the flux of gamma rays reported by HAWC Collaboration can be explained by photo-hadronic interactions.

The next step in this work will be to model the broadband radiative emission from internal jets. Effects of the supercritical regime must be taken into account, as the radiation field can dominate the energy density in the jet at the scales of the binary system. Also, to have a complete radiative model of SS433 we have to calculate the emission from the other regions of the terminal jet. The application of this model to other supercritical X-ray binaries (e.g. ULXs) will be presented in a forthcoming communication.

Acknowledgements: The authors thank LOC and SOC for having selected this work for the 62a Reunión Anual de la Asociación Argentina de Astronomía.

References

Abell G.O., Margon B., 1979, *Nature*, 279, 701
 Abeyssekara A.U., et al., 2018, *Nature*, 562, 82
 Blundell K.M., et al., 2001, *ApJL*, 562, L79
 Brinkmann W., et al., 2007, *A&A*, 463, 611

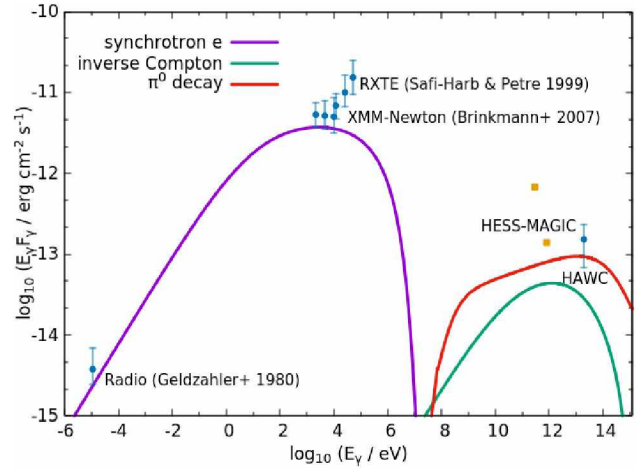


Figure 5: Spectral energy distribution of the radiation emitted. Observational data at different wavelengths are plotted.

Downes A.J.B., Pauls T., Salter C.J., 1981, *A&A*, 103, 277
 Dubner G.M., et al., 1998, *AJ*, 116, 1842
 Eikenberry S.S., et al., 2001, *ApJ*, 561, 1027
 Elston R., Baum S., 1987, *AJ*, 94, 1633
 Fabrika S.N., 1993, *MNRAS*, 261, 241
 Fabrika S.N., Abolmasov P.K., Karpov S., 2007, V. Karas, G. Matt (Eds.), *Black Holes from Stars to Galaxies – Across the Range of Masses*, *IAU Symposium*, vol. 238, 225–228
 Geldzahler B.J., Pauls T., Salter C.J., 1980, *A&A*, 84, 237
 MAGIC Collaboration, et al., 2018, *A&A*, 612, A14
 Margon B., 1984, *ARA&A*, 22, 507
 Marshall H.L., Canizares C.R., Schulz N.S., 2002, *ApJ*, 564, 941
 Mirabel I.F., Rodríguez L.F., 1994, *Nature*, 371, 46
 Paragi Z., et al., 2002, *Proceedings of the 6th EVN Symposium*, 263
 Reynoso M.M., Medina M.C., Romero G.E., 2011, *A&A*, 531, A30
 Reynoso M.M., Romero G.E., Christiansen H.R., 2008, *MNRAS*, 387, 1745
 Romero G.E., Vieyro F.L., Vila G.S., 2010, *A&A*, 519, A109
 Romero G.E., Vila G.S., 2008, *A&A*, 485, 623
 Safi-Harb S., Ögelman H., 1997, *ApJ*, 483, 868
 Safi-Harb S., Petre R., 1999, *American Astronomical Society Meeting Abstracts*, vol. 193, 125
 Shkrovskii I.S., 1981, *Soviet Ast.*, 25, 315
 Sotomayor Checa P., Romero G.E., 2019, *A&A*, 629, A76